Proceedings of the 28th IEEE
EMBS Annual International Conference
New York City, USA, Aug 30-Sept 3, 2006

A Parallel FDTD Scheme for Electromagnetic Analysis and Design of MRI System

Hua Wang, Adnan Trakic, Ling Xia, Stuart Crozier, *Member, IEEE*, Feng Liu and Marek Bialkowski, *Fellow, IEEE*

Abstract — **This paper presents a parallel-computing FDTD simulator for electromagnetic analysis and design applications in Magnetic Resonance Imaging system. It is intended to be a complete, high-performance FDTD model of an MRI system including all temporal RF and low-frequency field generating units and electrical models of the patient. The developed MRI-dedicated FDTD algorithm is adapted to a parallel computing architecture with the MPI library. Its capabilities are illustrated in two distinct, large-scale field problems. One concerns the interaction of RF-fields with human tissue at high magnitude fields. The other includes the characterization of the temporal eddy currents induced in the cryostat vessel during gradient switching. The presented examples demonstrate the computational efficiency and extended analyses available due to the parallel FDTD framework.**

I. INTRODUCTION

The Finite-Difference Time-Domain (FDTD) method is well suited to electromagnetic analyses in MRI applications, due to its simplicity and efficiency in wave modelling and its ability to handle field-sample interactions and nonlinear phenomena [1-2]. However, with the recent evolution of MRI towards high field strengths, the complicated interaction of electromagnetic fields with the patient and resistive MRI components requires more sophisticated large-scale-high-resolution (LSHR) algorithms with increased computing performance.

In recent years we have developed a series of single-processor based FDTD schemes [3-10], which can be employed to analyze modern MRI problems over a wide range of operating frequencies. Our long term aim is to generate a complete temporal FDTD model of an MRI system including all the field generating units and an electrical model of a patient. A better understanding of the complex temporal interaction of the fields within the patient and the MRI system components during an MRI scan can provide useful insight into the coil design. However, in the realm of LSHR computing, the single processor based methods are limited and often incapable of managing large memory and computational time requirements. Therefore, to improve the performance the FDTD scheme, it is necessary to further explore computational strategies such as parallelization.

The FDTD method and related hybrid algorithms, based on their geometrical topology, are highly adaptable to the parallel computing framework, in which the computing task is divided and assigned to many processors with distributed or shared memory allocations. With parallel computing supported by MPI library *herein*, field problems in MRI that require considerable memory resources can be solved much faster than using a single processor approach. Subsequently, in this work we implement MRI-dedicated cylindrical and Cartesian parallel FDTD schemes, which can be applied to different system geometries under a wide range of frequencies. The cylindrical FDTD method is demonstrated for the analysis of a low frequency (LF) problem, *i.e.*, transient eddy currents in the cryostat induced during switching of a transverse gradient coil. The Cartesian FDTD method is parallelized for the comparative study of the interactions of RF-fields with male/female human models. The problems are treated with high spatial resolution, which is beyond the capability of the conventional non-parallelized FDTD algorithms. The simulation results indicate the enhanced performance of the developed FDTD simulator.

II. METHODOLOGY

A. Cartesian and cylindrical FDTD methods

The Maxwell's equations can be expressed in Cartesian or cylindrical coordinate systems with components of the magnetic (H) and electric field (E) intensity formulated in a general form [11] as given by the following expressions:

$$H_A\big|_{i,j+1/2,k+1/2}^{n+1/2} = C_{h1} H_A\big|_{i,j+1/2,k+1/2}^{n} + C_{h2}\left(\frac{E_B\big|_{i,j+1/2,k+1}^{n} - E_B\big|_{i,j+1/2,k}^{n}}{\Delta C} - \frac{E_C\big|_{i,j+1,k+1/2}^{n} - E_C\big|_{i,j,k+1/2}^{n}}{r_i \Delta B}\right)$$

$$E_A\big|_{i+1/2,j,k}^{n+1} = C_{e1} E_A\big|_{i+1/2,j,k}^{n} + \frac{\Delta t}{\varepsilon} J_A\big|_{i+1/2,j,k}^{n+1/2} + C_{e2}\left(\frac{H_C\big|_{i+1/2,j+1/2,k}^{n+1/2} - H_C\big|_{i+1/2,j-1/2,k}^{n+1/2}}{r_{i+1/2}\Delta B} - \frac{H_B\big|_{i+1/2,j,k+1/2}^{n+1/2} - H_B\big|_{i+1/2,j,k-1/2}^{n+1/2}}{\Delta C}\right)$$

where $A=x(or\ r)$, $B=y(or\ \phi)$ and $C=z$ for Cartesian (cylindrical) coordinates $\Xi = (A,B,C)$. The variable r_ξ ($\xi \in \{i,i+1/2,i-1/2,i+1,i-1\}$) is the radial displacement employed in the cylindrical FDTD method. For the Cartesian FDTD method, $r_\xi = 1$ for all values of ξ. In the discrete FDTD computational domain, the dimensions of the Yee cell are defined by ΔA, ΔB and ΔC. The relative permeability $\mu(\Xi)$, relative permittivity $\varepsilon(\Xi)$ and conductivity $\sigma(\Xi)$ are defined at the center of the cell. Parameter J_Ξ represents the

impressed current density [in Am^{-2}]. During updating of E-field components, coefficients are linear for the RF problem case and nonlinear for modelling of exponential decay of propagating waves inside conductors. In low frequency (LF) applications, the conventional FDTD method suffers from prohibitively long computational time [3]. To overcome this problem, the weakly coupled Maxwell's equations can be adapted to the LF regime by downscaling the speed of light constant, which permits the use of larger time steps while maintaining the validity of the CFL stability condition. In our recent study, this modification has been accomplished by scaling up the permittivity of free space ε_0 by a scaling factor α: $\varepsilon = \varepsilon_r(\alpha\varepsilon_0)$.

In the cylindrical formulations, numerical singularity associated with the polar axis (r = 0), needs to be considered. A series expansion provides an approximation in the radial direction that satisfies some regularity conditions [8].

B. Parallel computing architecture

The aforementioned FDTD algorithms can be easily adapted to parallel architecture with the MPI library. With its reputed stability, optional communication routines and robust compatibility, MPI is considered to be one of the prominent environments to support parallel computing.

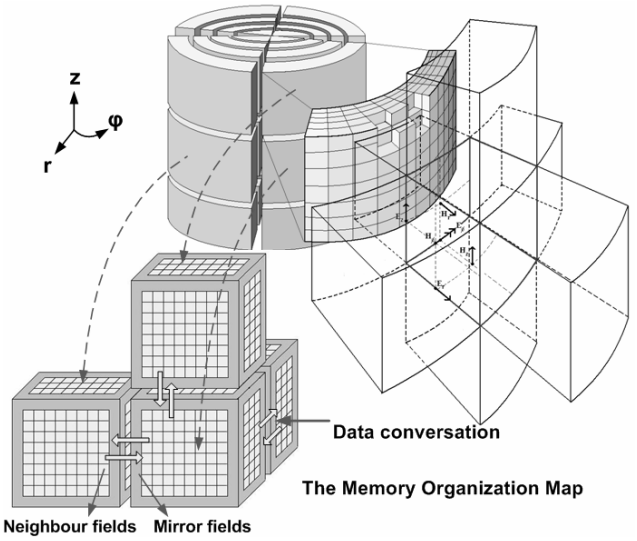

Fig. 1. – Arrangement of electromagnetic field components in the cylindrical Yee cell with parallel computing framework and the message communication routine mechanism for parallel FDTD.

In FDTD, the problem space has to be specifically defined before field calculations. In parallel framework, the computational space is divided into several domains of approximately equal size (see Fig.1) and each domain is managed by one process. All processes run on several processors executing the same program, while each process operates on memory that is allocated to it. As a result, mutual access to the memory is not straightforward. The data conversation between the neighbour processes exchanges the EM fields to keep them continuous over the unified domain.

The FDTD execution procedure is shown in Fig.2. Initially all field values are set to zero or a known initial value. Next,

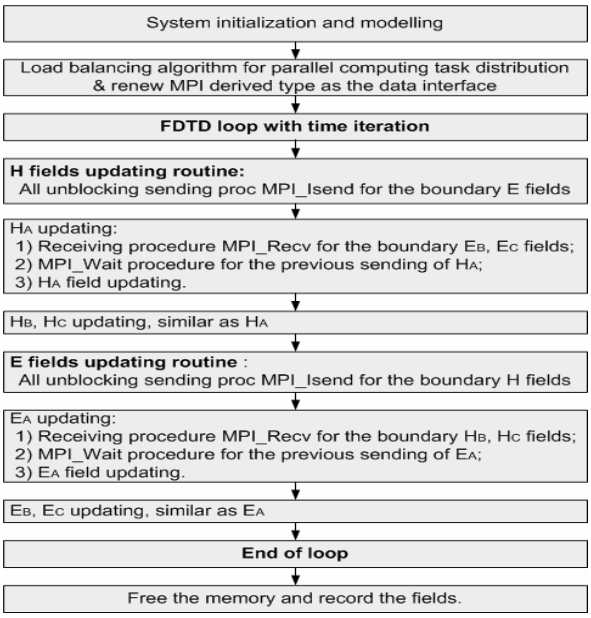

Fig. 2. – The processing flow of FDTD with unblocking message communication parallelism.

the load balancing algorithm is utilized to evaluate the optimized solution for scale distribution. As the major step, a looping procedure starts to discretely solve the EMFs at time increments. The output data is organized and analyzed in a post-processing module. In the undertaken implementation, before using the FDTD solver, all the system parameters such as human model and source data are obtained from files. For each cell, the associated properties such as cell type, electrical parameters and even updating coefficients are obtained and indexed by pointers. Before FDTD iterations, setting the neighbor status is required to further accelerate the updating procedure of all EMF components. The E-H fields are then collected from sub-processes for the later analyses.

III. FDTD APPLICATIONS

The application and performance of the parallel computational structures are demonstrated using a 3-server cluster network, each with 2 XEON 3.6 GHz processors and 4 GB of memory, which are coded by the standard MPI library and managed by MPICH parallel computing platform.

A. RF application using Cartesian FDTD

In the first example, the analysis of the interaction of RF fields with human body is carried out by applying the parallel FDTD method in Cartesian coordinates. Inhomogeneous 2mm-resultion numerical voxel phantoms of a male (Norman, 277x148x871 voxels) and a female human subject (Naomi, 294x124x791) [12, 13] are employed to compute the Specific Absorption Rate (SAR) due to a whole-body quadrature polarized 16 rung birdcage resonator, operating at 340MHz. The space domain enclosing the birdcage resonator, PML-layers and the human phantom are modelled with 354×354×914 cells in the male and 354×354×842 cells in the female phantom. The dielectric properties of all

body-identified tissue types are frequency scaled and kept constant at 340MHz [12]. The input power of birdcage resonator is numerically adjusted to provide a 90-degree flip angle for most of the tissue in the chest and abdominal region for both male and female numerical models. In the FDTD computational process the time stepping is performed for about six sinusoidal cycles before reaching the steady state, followed by evaluation of SAR values.

B. Low frequency application using Cylindrical FDTD

In the second example, which concerns the use of the parallel FDTD in cylindrical coordinates, the induced LF transient eddy currents are computed and analysed in the cryostat and radiation shield walls caused by pulsing of an actively shielded, symmetric, whole-body transverse y-gradient coil. The choice of the '*c*-downscaled' FDTD scheme in cylindrical coordinates [9] is motivated by a lower staircase error for the transverse coil and secondary fields in the conducting components of the MRI system than the FDTD method in Cartesian coordinates. With a current magnitude of 100A, the y-gradient coil is designed to generate a linear magnetic field gradient of 10mT/m in the Diameter Spherical Volume (DSV, 50cmX50cm). The gradient coil is 1.28m in length, whereby the primary and secondary layers are radially 0.345m and 0.425*m* away from the central z=0 axis, respectively. The frequency and current rise time of the trapezoidal current excitation are 500 *Hz* and 250μs. Thus the *dB/dz/dt* value for both systems is approximately 40 $mTm^{-1}s^{-1}$.

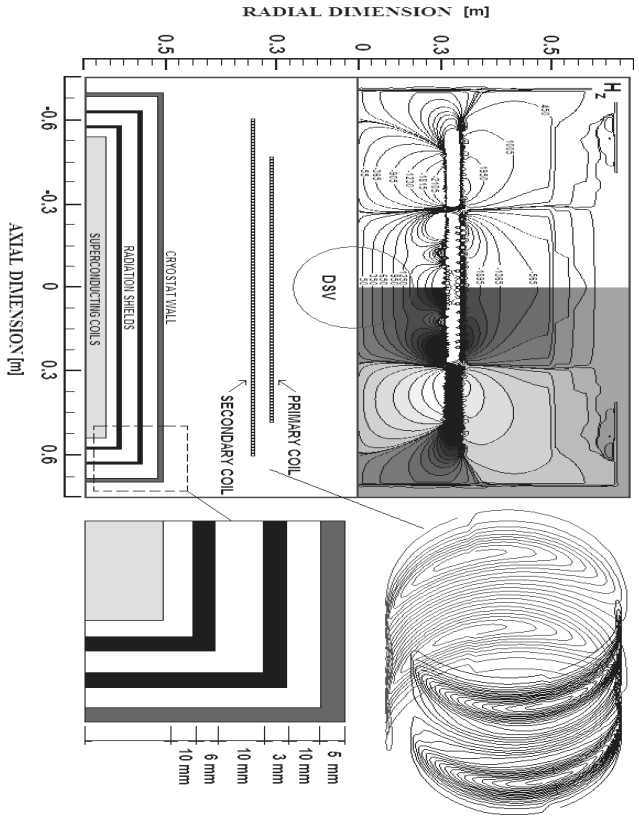

Fig. 3. – System setup for the y-gradient coil indicating the dimensions used and the snapshot of spatial axial magnetic field strength in the system illustrating a homogeneous field in the working volume.

We initially consider a 5mm-thick/1.4m-long stainless steel cylindrical cryostat and aluminium radiation shield walls. The cryostat and radiation shield walls have inherent material conductivities of around $2e^6$ $Sm^{-1}$and $2e^7$ Sm^{-1}, respectively. Magnetic linearity is assumed throughout the problem domain. The grid resolution in axial and azimuthal dimension is same in the whole problem domain: $\Delta z=5mm$ and $\Delta\varphi=\pi/180$, $\Delta r=5mm$ *in air and* $\Delta r=0.5mm$ *in* cryostat and radiation shield walls.

Fig. 3 illustrates the overall system set-up for the symmetric y-gradient coil and surrounding cryostat and radiation shield walls. With a scaling factor and safety coefficient of $1e^{10}$ and 0.95 respectively, the time step Δt was around $2.605e^{-9}s$. The total number of iterations for a single gradient pulse (half period) was 383,891.

IV. RESULTS AND DISCUSSION

For the RF field-tissue interactions, Fig. 4 compares the values of SAR induced in the male and female subject in coronal, sagittal and axial planes. The simulation results indicate that a somewhat higher SAR values are induced in the Naomi than in the Norman model, especially in the abdominal

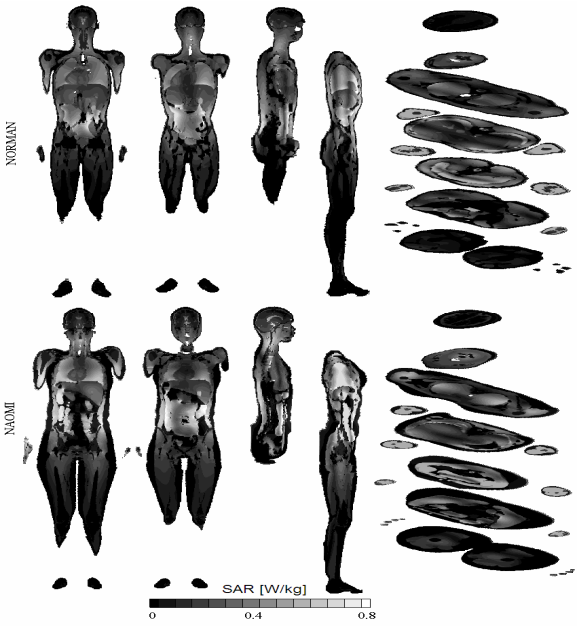

Fig. 4. – Comparison of normalized SAR distribution between Norman and Naomi in axial, sagittal and coronal view.

region. The discrepancy in the simulation results is primarily due to the dissimilar physiological structure. As expected, peak SAR values are localized in the chest/abdominal region for both the male (0.71 W/kg) and female model (0.83 W/kg). The computational times for the Norman and Naomi phantoms were approximately 3.5 and 3.7 hours, respectively.

In the LF application involving the y-gradient coil, we demonstrate the use of the proposed parallel FDTD scheme in the analysis of magnetic field diffusion and induction of eddy currents in nearby conducting structures when pulsing magnetic field gradients. Variable cell size technique for

FDTD is engaged in this design, which ensures high resolution of eddy current analysis in the radiation shields, as accurate as 0.5mm. Fig. 3 presents the field snapshot of the axial magnetic field in the r-z-plane at t=50μs, which illustrates the gradient field uniformity in the working volume. Fig. 5 shows the spatial normalized azimuthal electric field due to eddy currents in the cryostat and radiation shields for a single gradient pulse of 40 *mT/m/s*. The cryostat wall attenuates most of the field before it is incident on the radiation shields. Since

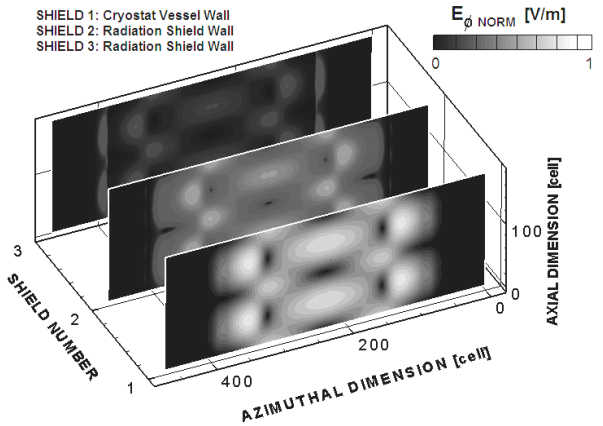

Fig. 5. – The spatial normalized azimuthal electric field due to eddy currents at the inner surface of the cryostat and radiation shield walls

the shielding coil is closer to the cryostat vessel than the primary coil, the coil pattern of the secondary coil can have a significant effect on the spatial eddy current distribution in the cryostat and radiation shield walls. According to the specific hardware setting *herein*, the devised parallel routine on the cluster network of processors was approximately ten times faster than when a single processor was used. Via the above analysis on the optimized schemes, the parallel computing FDTD structure shows a robust performance. Also, with the more accurate description of curved gradient coils and cryostat/radiation shield assembly in the cylindrical coordinates, the whole MRI system can be modeled with this parallelism.

From the above case studies, it can be seen that the developed simulator allows for analysing a wide range of MRI-related field calculation problems; with the enhanced computational power. It can also be used to test new designs and prototypes development. For example, inverse design of high frequency RF coils [14] with the consideration of loading effect could be a challenge to this parallel FDTD framework. Some novel transceiver protocols for high field MRI can also be tested before practical tests take place.

V. CONCLUSION

Computationally intensive numerical software has become necessary to handle the increasing complexity of EMF problems in MRI, particularly at high field strengths. In this work, a dedicated, high performance FDTD simulator architected with parallel framework has been presented. The potential of the optimized parallel FDTD scheme has been demonstrated in two typical MRI applications. The case studies indicate that the power of the software enables straightforward adaptation to applications involving optimization of system components. It has been illustrated that parallel computing can increase the computational efficiency and power in large-scale, high-resolution numerical problems, which could have a significant impact in the design and evaluation of MRI subsystems. By enabling the parallel FDTD simulations, as shown in this work, we are in a position to approach a complete transient model of an MRI system, including detailed tissue-field interactions and the effect of electromagnetic fields on surrounding coils/conductors.

ACKNOWLEDGMENT

Financial support of the Australian Research Council for this project is gratefully acknowledged. Also acknowledged is Dr. P. J. Dimbylow (NRPB, UK) for providing the numerical models of the male and female human phantoms.

REFERENCES

[1] C.M. Collins, S. Li, M.B. Smith, SAR and B1 field distributions in a heterogeneous human head model within a birdcage coil, Magn. Reson. Med. 40 (1998) 847-856.

[2] T.S. Ibrahim, R. Lee, B.A. Baertlein, Y. Yu, P.M.L. Robitaille, Computational analysis of the high pass birdcage resonator: finite difference time domain solutions for high-field MRI, Magn. Reson. Imag. 18 (7) (2000) 835-856.

[3] F. Liu, S. Crozier, H. Zhao, Finite-difference time-domain based studies of MRI pulsed field gradient-induced eddy currents inside the human body, Concepts Magn. Reson. 15 (B1) (2002) 26–36.

[4] H. Zhao, S. Crozier, F. Liu, A FDTD method for modeling the effect of switched gradients on the human body in MRI, Magn. Reson. Med. 48 (2002) 1037–1042.

[5] H. Zhao, S. Crozier, F. Liu, An analysis of the high-definition finite-difference time-domain methods, Appl. Math. Model 27 (2003) 409–419.

[6] F. Liu, S. Crozier, A distributed equivalent magnetic current based FDTD method for the calculation of E-fields induced by gradient coils, J. Magn. Reson. 169 (2004) 323–327.

[7] Q. Wei, F. Liu, L. Xia, S. Crozier, An object-oriented designed finite-difference time-domain simulator for electromagnetic analysis and design in MRI – applications to high field analyses, J. Magn. Reson. 172 (2005) 222-230.

[8] F. Liu, S. Crozier, An FDTD Model for calculation of gradient induced eddy currents in MRI system, IEEE Trans. Appl. Superconduct. 14 (2004) 1983–1989.

[9] A. Trakic, H. Wang, F. Liu, H. S. Lopez and S. Crozier, Analysis of Transient Eddy Currents in MRI using a Cylindrical FDTD method, IEEE Trans. Appl. Superconduct. [in press 2006]

[10] F. Liu, B.L. Beck, B. Xu, J.R. Fitzsimmons, S.J. Blackband and S. Crozier, Numerical modelling of 11.1T MRI of a human head using a MoM/FDTD method, Concepts Magn. Reson. 24(B1) (2005), 28-38.

[11] K.S. Yee, Numerical solution of initial boundary value problems involving Maxwell's equations in isotropic media, IEEE Trans. Antennas Propagation.,14 (1966) 302-307.

[12] P.J. Dimbylow, Current densities in a 2 mm resolution anatomically realistic model of the body induced by low frequency electric fields, Phys. Med. Biol. 45 (2000) 1013-1022.

[13] P.J. Dimbylow, Development of the female voxel phantom, NAOMI, and its application to calculations of induced current densities and electric fields from applied low frequency magnetic and electric fields, Phys. Med. Biol. 50 (2005) 1047–1070.

[14] B.G. Lawrence, S. Crozier, D.D. Yau and D.M. Doddrell, A time-harmonic inverse methodology for the design of RF coils in MRI, IEEE Trans. Biomed. Eng., 49 (2002) 64-71.